First Estimates of the Diurnal Variation of Longwave Radiation from the Multiple-Satellite Earth Radiation Budget Experiment (ERBE)

Edwin F. Harrison,[1] David R. Brooks,[1] Patrick Minnis,[1] Bruce A. Wielicki,[1] W. Frank Staylor,[1] Gary G. Gibson,[2] David F. Young,[2] Frederick M. Denn,[2] and the ERBE Science Team[3]

Abstract

First results for diurnal cycles derived from the Earth Radiation Budget Experiment (ERBE) are presented for the combined Earth Radiation Budget Satellite (ERBS) and NOAA-9 spacecraft for April 1985. Regional scale longwave (LW) radiation data are analyzed to determine diurnal variations for the total scene (including clouds) and for clear-sky conditions. The LW diurnal range was found to be greatest for clear desert regions (up to about 70 $W \cdot m^{-2}$) and smallest for clear oceans (less than 5 $W \cdot m^{-2}$). Local time of maximum longwave radiation occurs at a wide range of times throughout the day and night over oceans, but generally occurs from noon to early afternoon over land and desert regions.

1. Introduction

The energy balance of the earth as viewed from space has been of interest since the beginning of the era of earth-orbiting satellites. The Earth Radiation Budget Experiment (ERBE) presents the first opportunity to measure the earth's radiant energy with identical instruments flying simultaneously on separate satellites (Barkstrom, 1984; Barkstrom and Smith, 1986). ERBE sensors on the NOAA-9 spacecraft and the shuttle-launched Earth Radiation Budget Satellite (ERBS) provide improved temporal sampling for studying the diurnal variability of regional radiative parameters over the globe (Harrison et al., 1983). The ERBS is in a 57° inclination, 600-km altitude orbit which, counting both ascending and descending nodes, precesses through all local hours at the equator in 36 days. NOAA-9 is in an 870-km altitude sun-synchronous orbit with nominal equatorial crossing times at 0230 and 1430 local solar time (LST).

The combined data sets from these two ERBE satellites provide significant improvement in temporal sampling capability over previous single satellites designed for measuring the earth's radiation balance.[4] Broadband shortwave (0.2 to 5.0 μm) and longwave (5.0 to 50.0 μm) data are obtained from the ERBE scanner instruments. The monthly mean diurnal variability of longwave radiant exitance (LWRE) using the first available ERBE data is examined in this paper. The ability of the ERBE measurement system to adequately sample diurnal variations on a monthly basis is verified with the aid of data from the Geostationary Operational Environmental Satellite (GOES). Examples are given to illustrate the diurnal variability of total and clear-sky regional longwave radiation.

2. Analysis

Data from ERBS and NOAA-9 for April 1985 are used to quantify the diurnal variation of longwave (LW) radiation. The analysis of these data involves several steps. Instrument counts for each measurement are converted to broadband radiance according to a series of calibration and global spectral correction coefficients (Smith et al., 1986). Then each pair of LW and shortwave radiances, or LW alone at night, is used in conjunction with a set of statistical models of radiance derived from Nimbus-7 ERB data (Taylor and Stowe, 1984) and a maximum likelihood estimator technique (Wielicki and Green, 1988) to identify the most probable cloud cover for ERBE measurements taken over a known geographical surface type. Geotypes are restricted to ocean, land, desert, coast, or snow, and the cloud cover categories are clear (0–5%), partly cloudy (5–50%), mostly cloudy (50–95%), and overcast (95–100%). Finally, scene-dependent spectral corrections to radiance are calculated using the ERBE scene classifications.

[1] Atmospheric Sciences Division, NASA Langley Research Center, Hampton, VA 23665-5225.

[2] Planning Research Corporation, Aerospace Technologies Division, Hampton, VA 23666.

[3] ERBE Science Team Principal Investigators: B. R. Barkstrom, ERBE experiment scientist and science team leader, Atmospheric Sciences Division, NASA Langley Research Center; R. D. Cess, State University of New York at Stony Brook; Y. Fouquart, LOA, University of Lille, France; A. Gruber, NOAA/NESDIS; D. L. Hartmann, University of Washington; F. B. House, Drexel University; R. S. Kandel, LMD/CNRS, Palaiseau, France; M. D. King, ERBE project scientist, NASA Goddard Space Flight Center; A. T. Mecherikunnel, NASA Goddard Space Flight Center; A. J. Miller, NOAA/NMC; V. Ramanathan, University of Chicago; J. Coakley, NCAR; E. Raschke, University of Cologne, Germany; G. L. Smith, NASA Langley Research Center; W. L. Smith, University of Wisconsin, Madison; and T. H. Vonder Haar, Colorado State University. A complete listing of ERBE Science Team members is given in Barkstrom (1984).

[4] For example, the Earth Radiation Budget (ERB) experiment on Nimbus-7 (Jacobowitz et al., 1984).

A scene- and geography-dependent limb-darkening model derived from Nimbus-7 (Taylor and Stowe, 1984) is used to calculate LWRE for each radiance. Each LWRE is then assigned to one of 24 local hours in one of 10,368 regions (2.5° latitude × 2.5° longitude). Values of LWRE obtained at the same local hour from both satellites are averaged; there are often overlapping measurements when the time of ERBS measurements coincides with that of the sun-synchronous NOAA-9. Even with a two-satellite ERBE data set, measurements can provide only a few estimates of LWRE during each day for a given region (Harrison et al., 1983). A complete monthly set of hourly LWRE for each 2.5° × 2.5° ERBE region is generally determined from linear interpolation between all measured LWRE values (Brooks et al., 1986). However, over land and desert regions, which have a large diurnal variation in radiant exitance, a half-sine model centered about local solar noon replaces the linear interpolation (under a set of restrictive criteria applied to the distribution and magnitude of LWRE data). Brooks and Minnis (1984) have shown that such a model is straightforward and can be applied to large numbers of ERBE measurements, consistently producing better diurnal averages (when compared with complete hourly sampling of simulated data) than, for example, simple or day length-weighted averages of daytime and nighttime measurements. The measured and modeled LWRE results in each 2.5° × 2.5° region are summed over the month to determine monthly hourly mean values.

Clear-sky sampling over land is often too sparse to permit day-by-day modeling or interpolation across all hours of the month. As an alternative, all clear-sky observations for each hour are accumulated during the entire month, and the monthly hourly clear-sky diurnal values are obtained from means of all the measured values at each hour. Nighttime LWRE is calculated as simply the mean of all the nighttime measurements. During the day, a trigonometric fit symmetrical about local solar noon (Brooks and Minnis, 1984) is applied to the data using the means (weighted by the number of measurements) at each local hour to determine the amplitude.

3. Results

Figure 1 illustrates the monthly mean hourly LWRE for the total scene (including clouds) over a high altitude desert region in South America during April 1985. The ERBE results are represented by the solid line, and it is clear that the general shape of the diurnal cycle could not be established with NOAA-9 data alone, which are centered at 0230 and 1430 LST. The combined results show that the LWRE exhibits a strong diurnal cycle with a maximum of 305 W · m^{-2} near mid-day and a minimum value of 242 W · m^{-2} at night.

GOES data can be used to verify the adequacy of ERBE temporal sampling to obtain accurate monthly mean diurnal variations of LWRE. GOES provides hourly narrowband (10 to 12 μm) measurements that, with appropriate calibrations, can be converted to broadband radiances, and then to radiant exitances, according to the methods developed by Minnis and Harrison (1984a). The technique, which yields a single calibration curve averaged over all scenes, has an rms difference of 4%. The GOES results are also given in Fig. 1 (dashed line) and show a favorable comparison with ERBE that verifies both

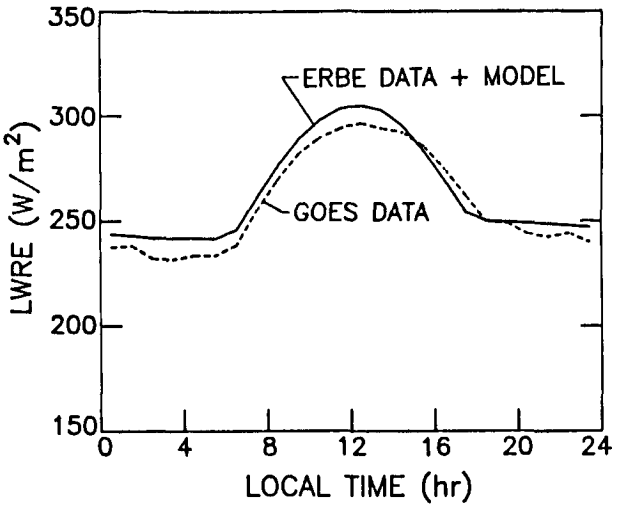

FIG. 1. Monthly mean diurnal variation of LWRE for ERBE (solid line) and GOES (dashed line) for a desert region in South America for April 1985 (latitude 21.25°S, longitude 68.75°W).

the monthly average LW calculation and the diurnal variation of the ERBE results. The differences between the two curves may be attributed to the persistent dry climate of the region (not an "average scene"), the limb-darkening models used to convert radiance to radiant exitance, the limited temporal sampling of ERBE, and the nature of the model used by ERBE for modeling the diurnal cycle for individual days.

In general, there are four major parameters of interest in studying global diurnal cycles of LWRE: diurnal range, times of maximum and minimum LWRE, and the integrated monthly average of the longwave radiation. The diurnal range of LWRE for each 2.5° × 2.5° region is defined simply as the difference between the maximum and minimum values of the monthly hourly mean LWRE in the region. Figures 2, 3, and 4 are examples of total and clear-sky LWRE diurnal results for selected regions with desert, land, and ocean backgrounds, respectively. The differences between the total and clear-sky data are due to the amount and types of cloud cover present over the region. Although the time of maximum total LWRE over desert and land tends to be somewhat biased toward noon because of the trigonometric model used in the averaging process, some interesting trends can still be observed in the results.

Figure 2 gives total scene and clear-sky LWRE diurnal results for the Atacama Desert region shown in Fig. 1. The large diurnal range (>60 W · m^{-2}) is typical of deserts and is in agreement with other data (e.g., Minnis and Harrison, 1984c). The total LWRE reached a maximum in early afternoon for the Atacama Desert. In addition, noon to early afternoon peaks observed for most land areas are consistent with other data (e.g., Hartmann and Recker, 1986). Diurnal range in LWRE over land is, however, considerably lower than the range over deserts. Early afternoon maxima generally occur over those deserts or land regions where convective cloud development is delayed until later in the day. Predominantly clear desert and land regions have maxima shortly after noon, indicating a slight lag of surface heating with insolation. The LWRE minima over these areas occur most often around sunrise since the surface is dominating the variation of LWRE.

Midmorning maxima in LWRE are found over high plateaus

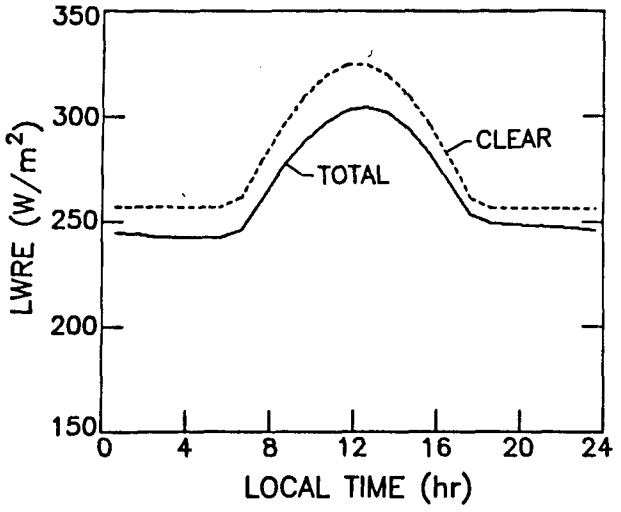

FIG. 2. Diurnal variation of LWRE for total scene (solid line) and clear-sky (dashed line) for the desert region in Fig. 1 from ERBE.

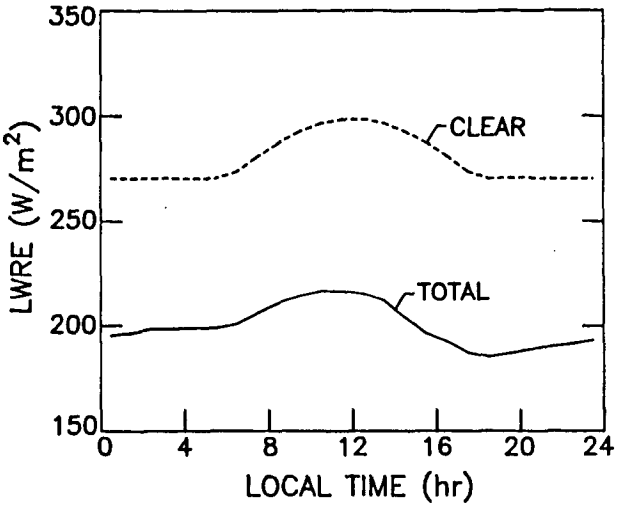

FIG. 3. Diurnal variation of LWRE for total scene (solid line) and clear-sky (dashed line) for a land region in the Amazon Basin of South America (latitude 3.75°S, longitude 66.25°W).

such as in central Africa and other highland areas in central and western Asia, Mexico, and the United States. Solar heating leads to cloud development earlier in the day over mountains. Convective activity occurs earlier in the day over mountainous areas than over adjacent lowlands. It is likely, therefore, that the late-morning cumulus cloud development over the highlands blocks the maximum solar heating of the surface at noon. A similar phenomenon taking place on a river-valley scale may be responsible for midmorning maxima seen over some lowlands in North America and much of tropical South America. Figure 3 shows diurnal results for a land region in the Amazon Basin of South America. The LWRE diurnal cycle for this region has a late morning maximum and a minimum shortly after sunset. The maximum before noon is consistent with an afternoon maxima in convective activity over the Amazon Basin (Minnis and Harrison, 1984b; Hartmann and Recker, 1986).

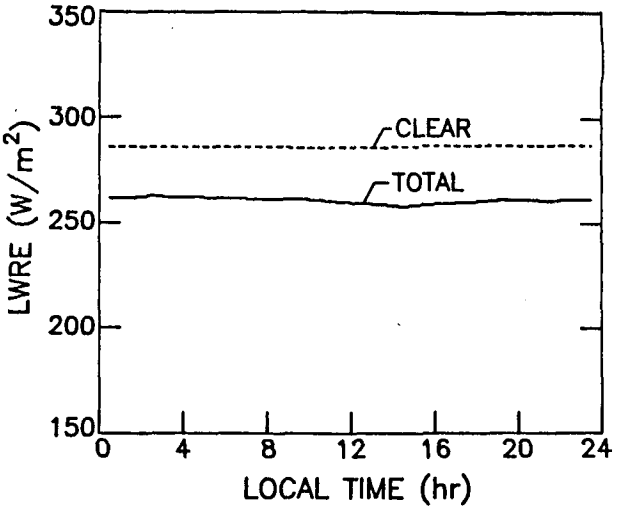

FIG. 4. Diurnal variation of LWRE for total scene (solid line) and clear-sky (dashed line) for a Pacific Ocean region (latitude 3.75°N, longitude 133.75°W).

The evening minimum is typical of tropical land areas. The warming after sunset is due to the dissipation of high clouds associated with diminished convective activity (Minnis and Harrison, 1984b, 1984c). The monthly mean LWRE is 200 $W \cdot m^{-2}$, which is consistent with the high, thick cloud cover associated with intense convective activity present in this area. The clear-sky LWRE of 279 $W \cdot m^{-2}$ is typical of warm equatorial regions. LWRE diurnal range is 32 $W \cdot m^{-2}$ for the total scene and 27 $W \cdot m^{-2}$ for clear sky.

The example of LWRE over oceans shown in Fig. 4 is for a region in the eastern Pacific just north of the equator. The diurnal range of LWRE is slightly less than 10 $W \cdot m^{-2}$, with a poorly-defined peak between midnight and sunrise and a mid-afternoon minimum. The frequent occurrence of maxima between midnight and 0800 LST over many ocean regions is consistent with the observed predominance of an afternoon maximum in high-altitude clouds (e.g., Minnis et al., 1987). Afternoon maxima in LWRE generally occur over marine areas that are mostly clear or have persistent stratocumulus cloud cover. This latter feature is most apparent off the western coasts of northern and southern Africa and South America. Cloud cover in these areas generally reaches a minimum during the afternoon, exposing more of the warmer surface (e.g., Minnis and Harrison, 1984b; Duvel and Kandel, 1985; Hartmann and Recker, 1986).

The global distribution of integrated monthly average of LWRE and its diurnal range are shown for April 1985 in Figs. 5 and 6, respectively. In each case the data shown are smoothed contour plots based on monthly means from 2.5° × 2.5° regions.

The variations in monthly average LWRE are primarily latitudinal in nature, with the warmest areas in the tropics and the coolest regions at the poles. There are notable deviations from this pattern, however, mainly in the subtropics. In particular, the effect of high cloud cover over the Amazon Basin, equatorial Africa, and Indonesia is evident in the lower LWRE values for these regions. Low values of LWRE also define the high altitudes of the Tibetan Plateau. The major desert areas and the equatorial Pacific ITCZ are also distinguishable by the

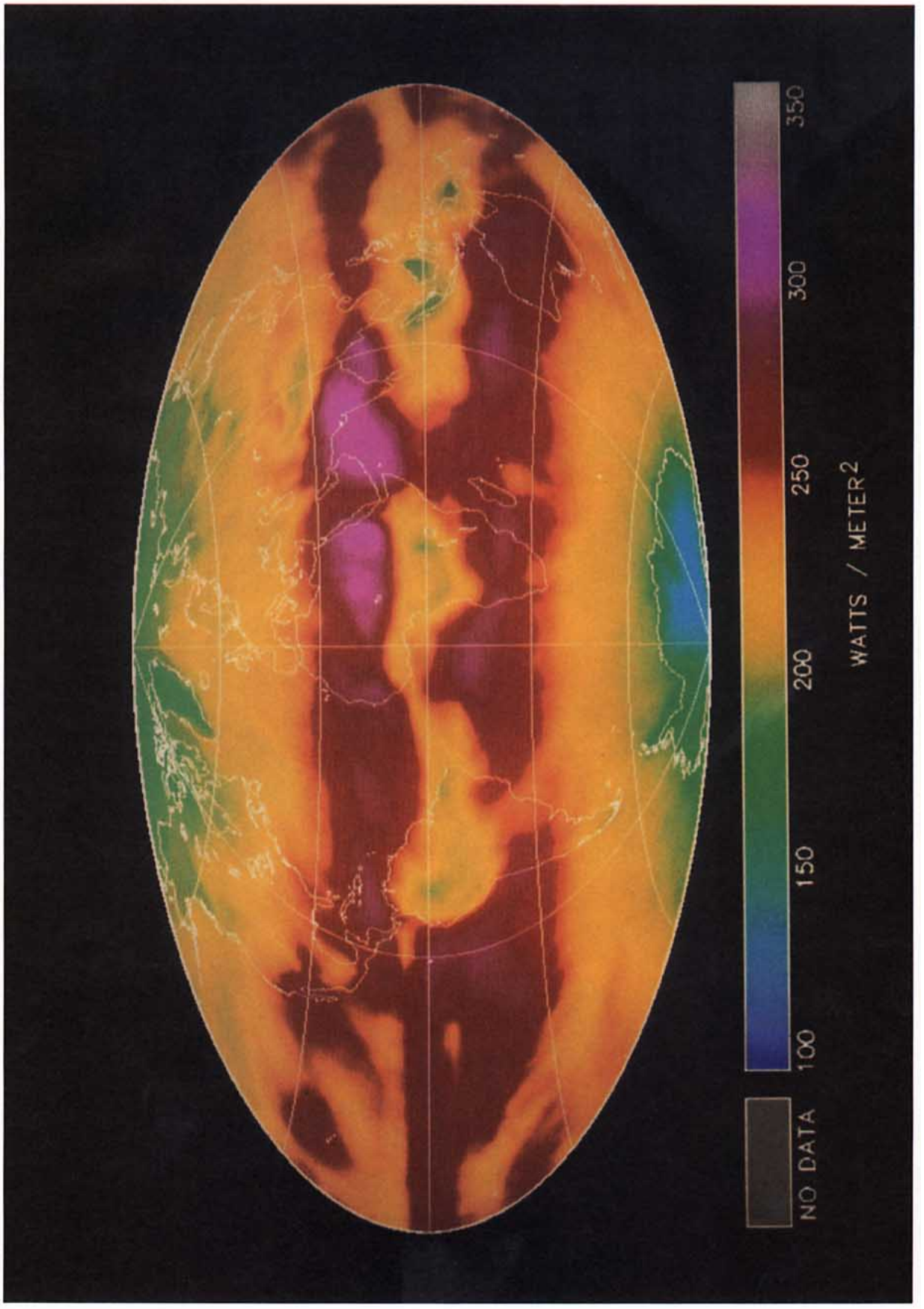

FIG. 5. ERBE monthly mean LWRE for April 1985.

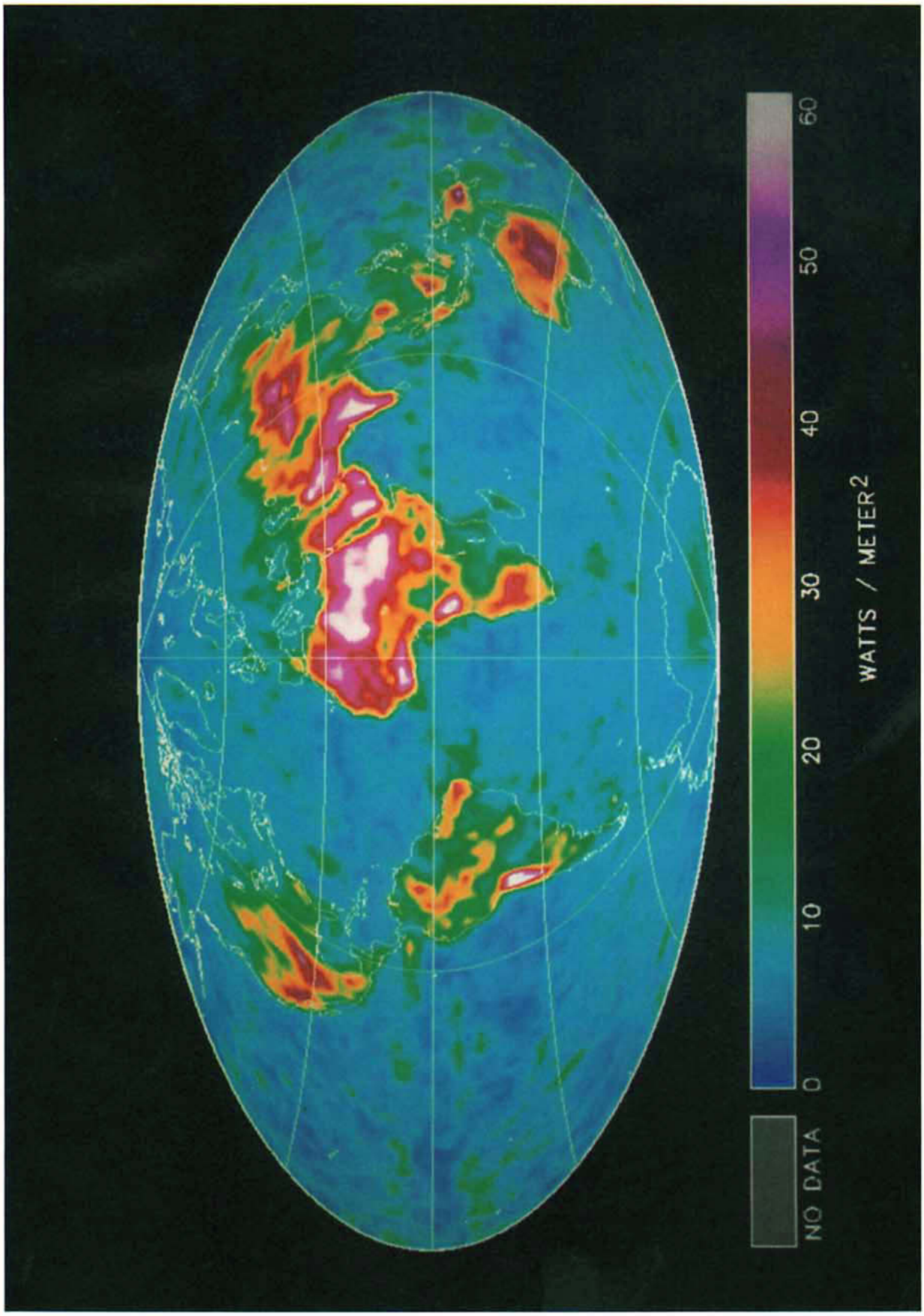

FIG. 6. Diurnal range of LWRE from ERBE for April 1985.

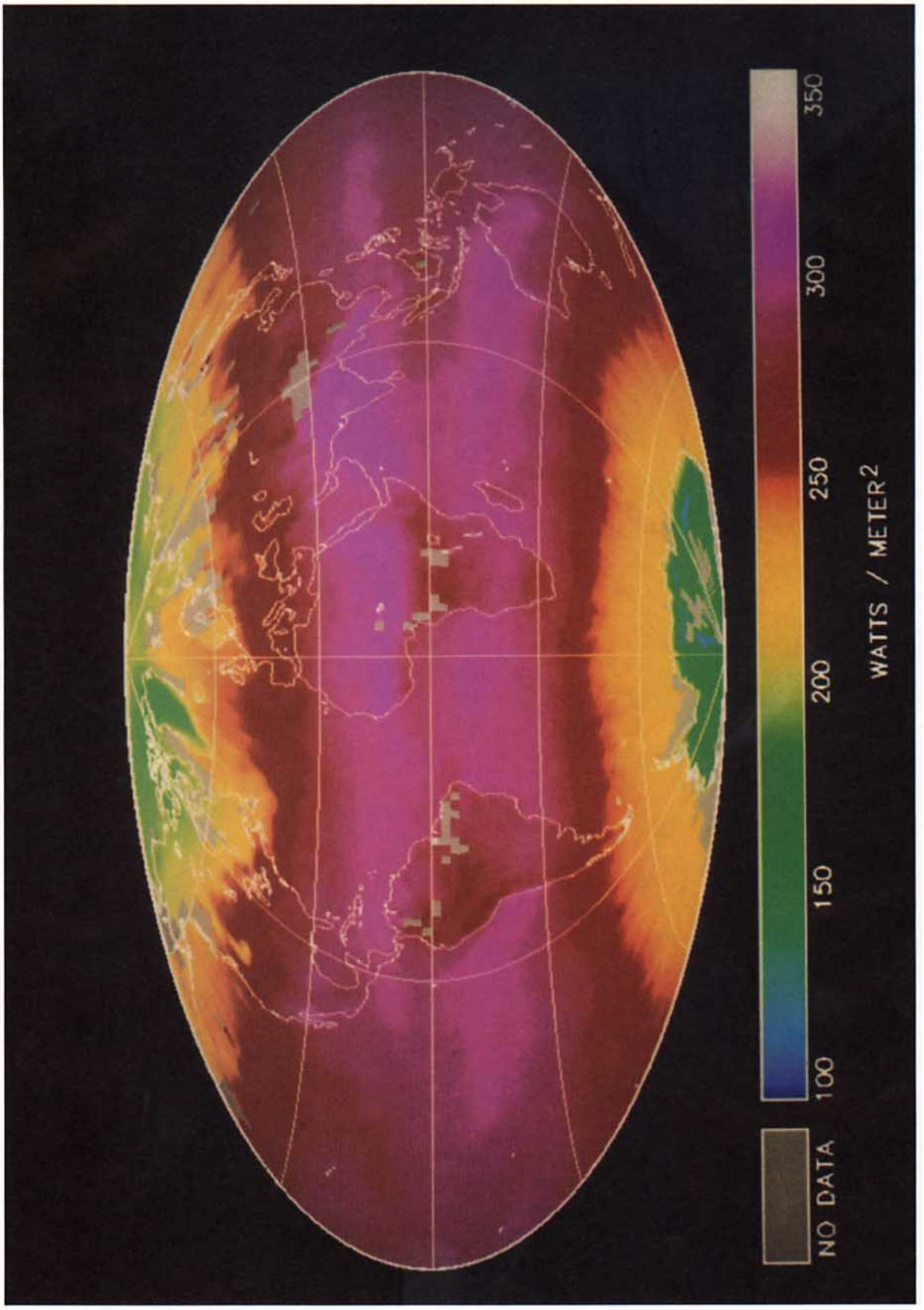

FIG. 7. ERBE monthly mean clear-sky LWRE for April 1985.

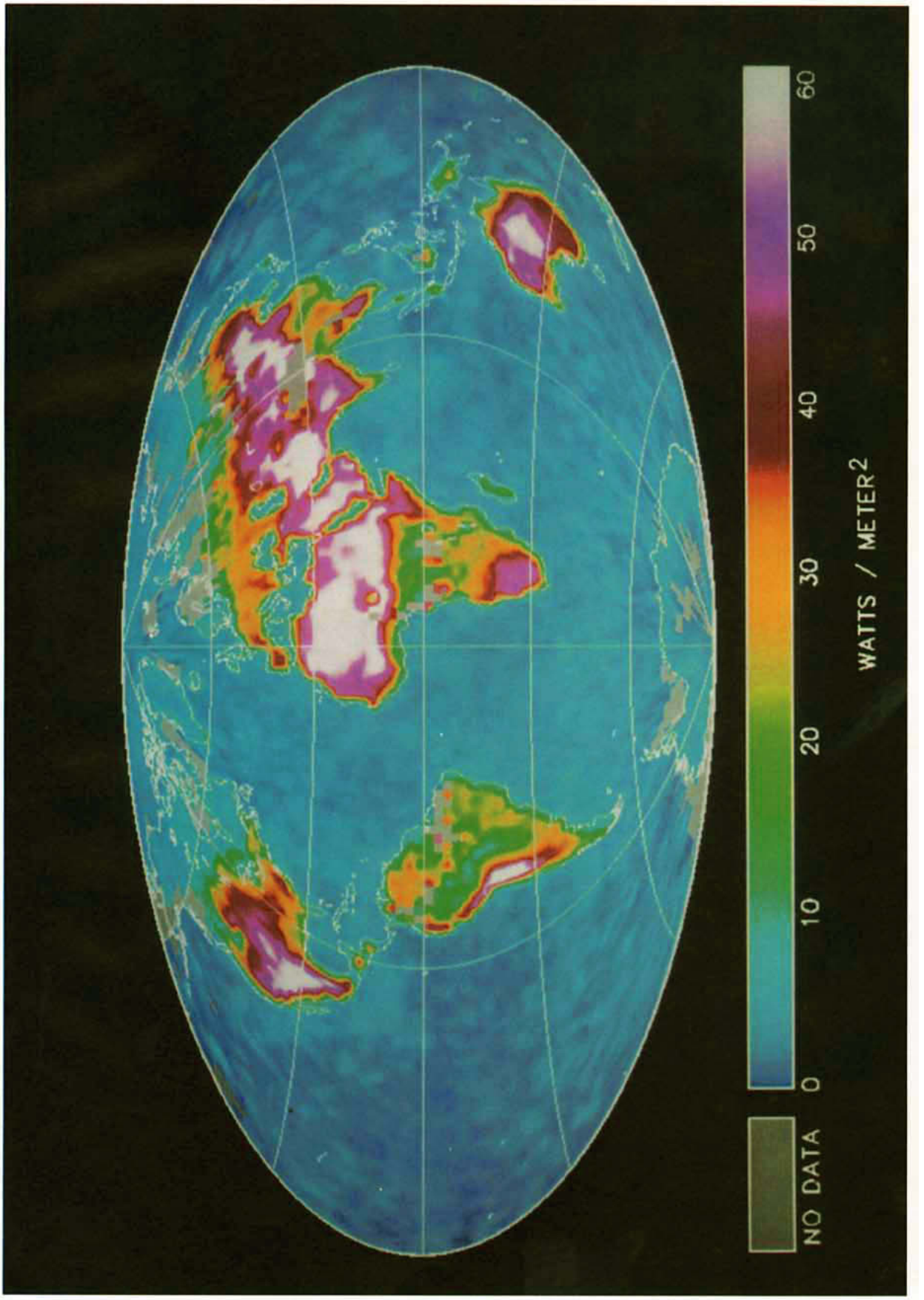

FIG. 8. Diurnal range of clear-sky LWRE for April 1985.

higher LW radiation that is seen in regions having very little cloud cover.

A global map of diurnal range is given in Fig.6. The patterns observed here can be related not only to the heating and cooling of the surface, but to diurnal changes in cloud amount and vertical structure. Because surface temperatures are relatively constant, diurnal variations in LWRE over oceans are primarily due to changes in cloudiness. Most of the tropical marine areas having a diurnal range greater than 10 W · m^{-2} also have a relatively low LWRE (see Fig. 4), indicating the presence of high clouds. The largest diurnal range of LWRE occurs in desert regions and over land areas, such as the Amazon Basin, that experience intense convective activity.

Monthly LWRE averages and the associated diurnal range for clear-sky conditions are shown in Figs. 7 and 8, respectively. Clear-sky monthly mean LWRE results outside the tropics show a zonal structure similar to the total scene LWRE averages. The magnitude of global clear-sky LWRE is generally greater by about 30 W · m^{-2}, since clouds reduce the amount of emitted longwave radiation at the top of the atmosphere. There are a few regions where clear-sky parameters could not be determined due to insufficient sampling or the continuous presence of cloud cover throughout the month. The geographical locations of regions not having clear-sky results are generally consistent with the cloud climatology of Warren et al. (1986), which shows a low frequency of clear skies over many of these areas during April. Clear-sky results over snow or ice backgrounds should be viewed with caution since it is extremely difficult to distinguish between cloudy and clear scenes in these regions.

Clear oceans have a very small diurnal variation in LWRE. Many land regions, notably deserts, exhibit extremely high diurnal variations of 50–75 W · m^{-2}. Similar results have been found by other researchers (Kandel, 1983; Minnis and Harrison, 1984c; Duvel and Kandel, 1985; Brooks, 1987). Moderate diurnal ranges of 20 to 40 W · m^{-2} are observed over typical vegetated land areas such as the eastern United States and large parts of South America.

4. Concluding remarks

Initial data from the Earth Radiation Budget Experiment have shown that many areas of the earth exhibit significant diurnal variations in longwave radiant exitance. The data indicate that global quantification of these variations benefits significantly from the availability of two satellites—one in a precessing orbit and the other in a sun-synchronous orbit. The areas having the largest diurnal range in longwave radiant exitance are typically deserts and land areas associated with intense convective cloud activity. Diurnal variations of ocean LWRE are smaller, ranging from less than 5 W · m^{-2} over clear oceans to about 15 W · m^{-2} over some cloudy ocean regions. From these initial ERBE data, it is clear that a considerable amount of new information about the global diurnal variations of radiation will become available with continued processing of the full ERBE data set. Utilization of these data in modeling and in empirical studies will lead to a better understanding of the role of one of the most basic cycles in weather and climate.

Acknowledgments. We would like to thank James F. Kibler of NASA Langley and the ERBE Data Management Team for their efforts in processing the ERBE data and making the appropriate data products available for scientific use. Computer programming support for producing the ERBE data output products was provided by Jack Paden and Jill Travers of OAO Corporation. Color graphics hardware and software support provided by Mark Shipham and Michelle Ferebee of NASA Langley is gratefully acknowledged.

References

Barkstrom, B. R., 1984: The Earth Radiation Budget Experiment (ERBE). *Bull. Amer. Meteor. Soc.*, **65,** 1170–1185.

Barkstrom, B. R. and G. L. Smith, 1986: The Earth Radiation Budget Experiment: Science and implementation. *Rev. Geophys.*, **24,** 379–390.

Brooks, D. R., 1987: Parameterized angular models for interpreting satellite-based measurements of shortwave and longwave radiances over deserts. Ph.D. dissertation, Imperial College of Science and Technology, University of London, 313 pp.

Brooks, D. R. and P. Minnis, 1984: Comparison of longwave diurnal models applied to simulations of the Earth Radiation Budget Experiment. *J. Climate Appl. Meteor.*, **23,** 156–160.

Brooks, D. R., E. F. Harrison, P. Minnis, J. T. Suttles, and R. S. Kandel, 1986: Development of algorithms for understanding the temporal and spatial variability of the Earth's radiation balance. *Rev. Geophys.*, **24,** 422–438.

Duvel, J. P. and R. S. Kandel, 1985: Regional-scale diurnal variations of outgoing radiation observed by Meteosat. *J. Climate Appl. Meteor.*, **24,** 335–349.

Harrison, E. F., P. Minnis, and G. G. Gibson, 1983: Orbital and cloud cover sampling analyses for multisatellite Earth radiation budget experiments. *J. Spacecraft and Rockets,* **20,** 491–495.

Hartmann, D. L. and E. E. Recker, 1986: Diurnal variation of outgoing longwave radiation in the tropics. *J. Climate Appl. Meteor.*, **25,** 800–812.

Jacobowitz, H., R. T. Tighe, and the Nimbus 7 ERB Experiment Team, 1984: The Earth radiation budget derived from the Nimbus 7 ERB experiment. *J. Geophys. Res.*, **89,** 4997–5010.

Kandel, R. S., 1983: Satellite observation of the Earth radiation budget. *Beitr. Phys. Atmosph.*, **56,** 322–340.

Minnis, P. and E. F. Harrison, 1984a: Diurnal variability of regional cloud and clear-sky radiative parameters derived from GOES data. Part I: Analysis method. *J. Climate Appl. Meteor.*, **23,** 993–1011.

Minnis, P. and E. F. Harrison, 1984b: Diurnal variability of regional cloud and clear-sky radiative parameters derived from GOES data. Part II: November 1978 cloud distributions. *J. Climate Appl. Meteor.*, **23,** 1012–1031.

Minnis, P. and E. F. Harrison, 1984c: Diurnal variability of regional cloud and clear-sky radiative parameters derived from GOES data. Part III: November 1978 radiative parameters. *J. Climate Appl. Meteor.*, **23,** 1032–1051.

Minnis, P., E. F. Harrison, and G. G. Gibson, 1987: Cloud cover over the equatorial eastern Pacific derived from July 1983 International Satellite Cloud Climatology Project data using a hybrid bispectral threshold method. *J. Geophys. Res.*, **92,** 4051–4073.

Smith, G. L., R. N. Green, E. Raschke, L. M. Avis, B. A. Wielicki, and R. Davies, 1986: Inversion methods for satellite studies of the Earth's radiation budget. *Rev. of Geophys.*, **24,** 407–421.

Taylor, G. R. and L. L. Stowe, 1984: Reflectance characteristics of uniform Earth and cloud surfaces derived from Nimbus-7 ERB. *J. Geophys. Res.*, **89,** 4987–4996.

Warren, S. G., C. J. Hahn, J. London, R. M. Chervin, and R. L. Jenne, 1986: Global distribution of total cloud cover and cloud type amounts over land. National Center for Atmospheric Research TN-273+STR, Boulder, CO.

Wielicki, B. A. and R. N. Green, 1988: personal communication. ●